Chapter 5

Dam-break flow against obstacles and through river bed singularities

Claude Marche
École Polytechnique de Montréal, Québec, Canada

Abstract

The consequences of a possible dam failure depend largely on the type of failure and the capacity of the reservoir it holds. However, riverbed singularities accumulate over the course of a flood and progressively take control. Fundamental characteristics of the riverbed progressively transform the dam-break wave and profoundly alter the shape of hydrographs and limnographs observed locally. These progressive changes in the dam-break wave are generally well identified by 1D and 2D numerical simulators commonly used for these calculations, including those that resolve only the kinematic form of St. Venant equations, for example. However, obstacles or very rapid changes in the physical characteristics of the bed channel are frequently present throughout the course of the dam-break wave. Over a very short distance, they may radically affect the wave's propagation and profoundly alter the scenario of the flood according to their characteristics, their sustainability or their progressive adaptation to flow conditions.

The existence of a natural or reservoir lake, the presence of an ice cover or a sand bar and the formation of debris jams in the path of a dam-break wave are frequent occurrences in rivers exposed to a rapid natural flood or a dam-break wave. A dam, a bridge, a road embankment and culvert are all examples of obstacles in a river that alter the dam-break flow dynamic over long distances. Their influence on potential consequences is very great.

These particular situations are specific to each river valley and require special attention. They often exceed the real possibilities of current numeric models.

1 The presence of a natural lake

It is common for a river to flow through one or several lakes along its course. When their surface is large, these bodies of water may have a decisive impact on natural flood routing and on the propagation of a potential dam-break flood wave. Dam failure generates a rise in water level and a temporary increase in the rate of flow to the receiving watercourse. The drowning rate diminishes slowly as the wave progresses downstream. It decreases significantly when the dam-break

WIT Transactions on State of the Art in Science and Engineering, Vol 36, © 2009 WIT Press
www.witpress.com, ISSN 1755-8336 (on-line)
doi:10.2495/978-1-84564-142-9/05

wave reaches the lake, which temporarily stores part of the excess volume of water received. Downstream from the natural outflow of the lake, the discharge transmitted to the river valley during the ascent phase of the flood is equal to that of the dam break minus the temporary retention exerted by the lake. The rise of the lake's water surface elevation will be as slow as the surface is large. It may also be diminished by the form of natural control of the outflow discharge. For all of these reasons, the dam-break wave exiting from a large natural lake may be very different from the wave entering the lake.

The system's hydrodynamic behaviour is generally described in the following routing equation (eqn. (1)) if the lake is of a regular shape, if it is of a maximum size of a few square kilometres and if the storage versus water surface elevation function is known based on the assumption that the surface is horizontal at all points in time (Anctil, [1]):

$$\frac{\Delta V}{\Delta t} = Q_{\text{in}} - Q_{\text{out}} \tag{1}$$

in which Δ is the differentiation symbol, V the actual lake volume, t the time variable, Q_{in} the instantaneous inflow discharge and Q_{out} the instantaneous outflow discharge.

However, considering the probable scale of the flood, this approach is rarely acceptable when studying dam failure. Resolution of a simplified or complete form of the St. Venant equations is preferable in order to obtain continuity of the liquid surface profile without iteration. In all cases, we observe that the system's dynamic depends mainly on five factors:

a) the distance between the dam and the downstream natural lake, resulting in preliminary attenuation of the wave as well as elongation;
b) the volume of the dam-break wave equal to the volume of water evacuated during the dam break, which determines the lake's peak elevation;
c) the duration of dam breach formation, which dictates the rate at which the water rises;
d) the lake's storage versus water surface elevation function and
e) The natural storage-outflow characteristics observed downstream from the lake as these two factors govern the lake's peak outflow discharge.

If the discharge rate of increase remains low, current numerical models based on the St. Venant equations are usually able to reproduce the phenomenon of flow attenuation and the progressive adjustment of the flood wave downstream from the lake. However, even in this case, calculations may lead to uncertain results if the potential storage of a lake or the outflow control are lesser known or inadequately reproduced by the model.

In the case of a 1D analysis, the user must ensure that cross-sections representing the river and the lake lead to adequate storage by using the model's interpolation functions. The calculated dam-break wave will be representative

of average flooding of the lake but will not factor in the secondary and often temporary effects associated with the direction of inflow or with the presence of a predominant channel in the lake. Above and beyond the maximum crest, these effects mainly influence the moment when local flooding begins.

Resorting to a 2D analysis enables factoring of local differences in water elevations throughout the lake. However, the results are only valid if the model adequately deals with variation in the horizontal surface of the water body as a function of the elevation in order to reproduce actual instantaneous storage.

If the flood's rate of rise is high, in addition to the above remarks, it will become necessary to use complete dynamic equations in order to detect the path of the wave front. These initial reflections will greatly affect instantaneous local elevations. As a rule, the peak stabilized elevation of the lake is not very sensitive to this dynamic aspect, which is significant only during the initial moments of the failure. However, it does result in another source of error, which stems from the non-permanent regimen of outflow control, lesser known as it depends simultaneously on local elevation and slope.

One final source of uncertainty is associated with the behaviour of the natural outflow itself. Previous calculations assume that the lake's outflow control refers to a section of the river, the shape of which remains stable throughout the flow of the dam-break wave. Such an assumption may be justified to simulate natural floods where the underwater portion of the control section presents an armour layer or proven resistance. The scale of a dam-break flood wave may greatly exceed that of natural floods and lead to instability of part of the control section (Zech and Spinewine, [2]). In such a case, the force of the dam-break wave that affects the watercourse downstream from the lake may be greater than predicted by calculation that assumes a fixed bottom: it may be intensified by draining part of the lake's content (Foda *et al.*, [3]). Only a detailed inspection of the outflow will provide the answer as to which scenario should be taken into account.

2 The presence of a downstream artificial lake

Although the effect produced on dam-break wave propagation by an artificial lake is similar to that of a natural lake, an artificial lake possesses a closure structure and control specifications that will affect the dynamic of dam-break flow differently. Result reliability when forecasting the consequences induced downstream depends on rigorous scrutiny of all possible scenarios as well as on the use of specific calculation capabilities.

Several artificial lakes hold large quantities of water thanks to structures that allow inflow and outflow management. Oftentimes, they have been established in such a way that they take maximum advantage of natural topographical depressions while controlling the outlet of the main watercourse with a dam. Lateral dikes prevent unwanted overtopping. The natural topography of certain regions (India, Pakistan and Northern Quebec, for example) is conducive to the construction and operation of such large-scale reservoir lakes (Marche, [4]).

The dynamic response of this type of reservoir to a very large inflow hydrograph caused by an upstream dam break will result in an increase in the water surface elevation of the reservoir, this large wave travelling from the point of entry to the farthermost boundaries of the reservoir. Overtopping of the embankments closest to the point of entry is likely to occur first. This will cause some alteration to the wave resulting in a diminished probability of damage to the main dam.

The evaluation of the safety and associated risks of this type of reservoir therefore rely, largely, on the reliability with which its response to a given catastrophic input may be modelled. It is possible, for example, that overtopping of a secondary dam could result in its failure, thereby reducing water surface elevations downstream and shielding other structures from any damage. Clearly, a simple mass conservation approach will often be inadequate because it assumes that the water surface in the reservoir remains horizontal at all instants in time (Singh and Li, [5]).

One-dimensional (1D) analyses applied along a longitudinal axis of the reservoir using dynamic wave assumptions together with the appropriate boundary conditions remains the most popular approximation used to treat the problem. However, this flow is often a two-dimensional phenomenon (2D) where the most significant effect is the appearance of a complex transverse curvature in the water surface elevation.

A comprehensive study of this type of singularity in dam-break wave propagation is given in Marche *et al.* [6]. It implies the use of a 2D dynamic dry bed model that is modified to play a role in the possibility of multiple failures by overtopping at various peripheral structures.

The specifically developed technique allows simulations of reservoirs even if they contain large islands or multiple channels. The technique has been validated in a laboratory setting using a physical model and applied to the safety study of structures and reservoirs on the La Grande River (Canada). Figure 1 shows a plan view of the LG3 reservoir and principal dikes. It also indicates the position of five points, the study of which will provide a better understanding of reservoir flow dynamic.

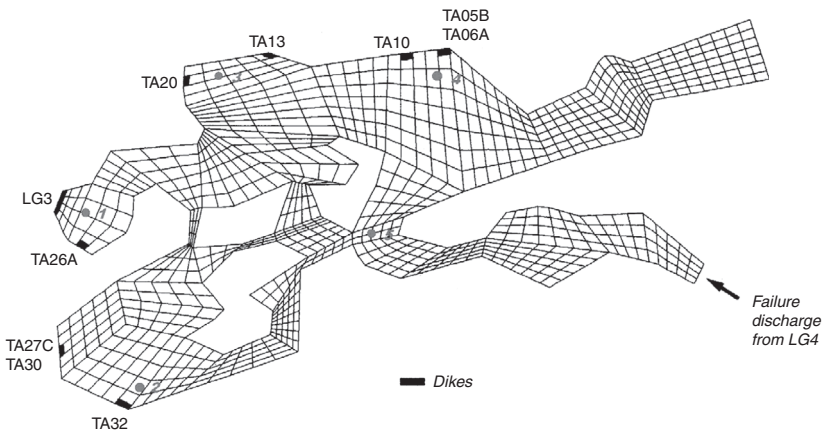

Figure 1: Plan view of the LG3 reservoir (Quebec).

Figure 2 refers to these points in order to demonstrate that local elevation in the reservoir is expected to show differences of several meters. Such differences greatly influence the sequence of failures in successive dams, the mode of dam-break wave propagation throughout the reservoir and the downstream valley flood process.

The velocity field calculated 13 hours after the upstream dam break is presented in fig. 3. At this point, failures at four main lateral dikes are already in progress.

Furthermore, the technique enables identification of the optimal functional specifications of lateral dikes if they are to be used as fuse plugs, a new

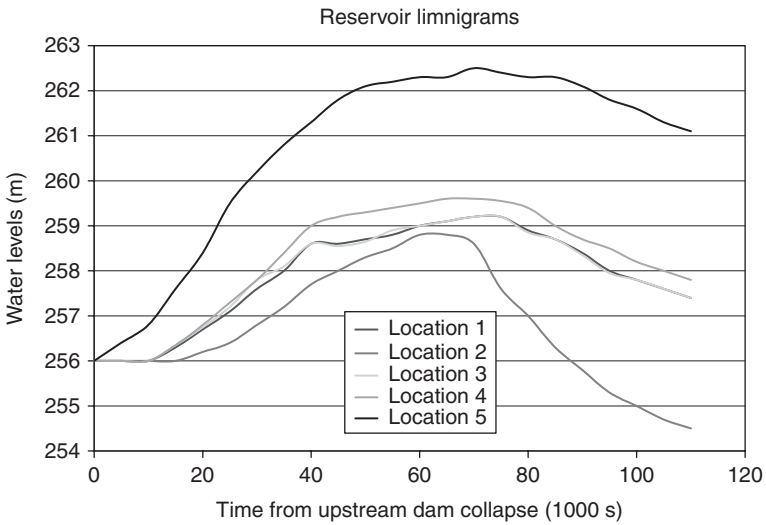

Figure 2: Variations in elevation in different areas of the reservoir.

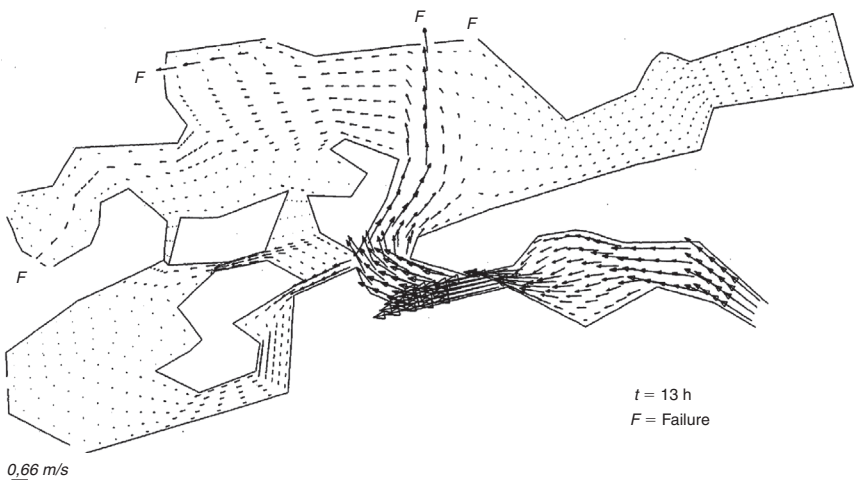

Figure 3: Identification of multiple failures.

concept recently introduced to increase safety at hydraulics facilities (Hakin, [7]; Marche *et al.*, [8]).

3 Presence of a sand bar at the mouth of the river

For many rivers, failure at a large dam would produce a flood, the impact of which would be felt as far as the sea or the ocean. Flood calculation and assessment of the possible consequences of such an event certainly implies a specific treatment of the estuary zone where it is vital to appropriately consider the effect of the tides. However, it may complicate forecasting when a sediment tongue, parallel to the coast, partially obstructs the estuary under the influence of littoral currents.

Figure 4 shows the Moisie River waterway into the St. Lawrence estuary and the scale of the partial obstruction exerted by the two bars. Available reports indicate that these points are constituted of fine to medium sand.

Certain areas of these bars are in constant motion and regularly affected by natural flooding. Under the influence of local tides in running water, the maximum outflow of this estuary may reach 1100 m^3/s. As a result of the tide's force versus river discharge, regular flow reversal can be observed in the greater part of the estuary.

The Moisie River flows from Labrador along a north–south course parallel to its neighbour, the Ste-Marguerite River. In conjunction with the SM3 dam, the high-capacity station is able to process the water from the Ste-Marguerite River as well as from the Careil and Aux Pékans rivers, which are natural tributaries of the Moisie. In order for the water to transfer from the Moisie basin to the Ste-Marguerite, two artificial reservoirs have been created by adding two substantial dikes, thus cutting

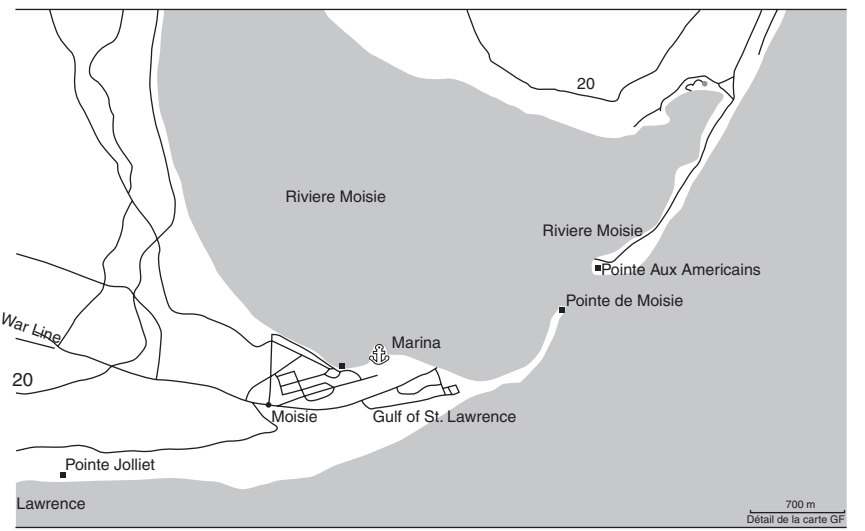

Figure 4: Plan view of the Moisie River estuary (Canada).

the former natural watercourses. However, the Moisie River, which has yet to be developed for hydroelectricity, is now susceptible to the risk of failure at the two diversion structures.

Calculations factoring in the possible failure of one or the other of these two embankments have been carried out using the classic 1D dynamic technique. These calculations predict flood wave propagation towards the estuary reaching a maximum discharge of approximately 24,600 m^3/s at one of the embankments. However, because of low storage capacity upstream from both embankments, return to a flow rate of 5000 m^3/s is expected within approximately 5 hours (Hydrocosme, [9]). Figure 5 shows the evolution of the flood wave discharge as it arrives upstream of the estuary zone.

Flood wave arrival in the estuary should be simulated according to two scenarios:

- The first takes into account the nearly instantaneous washing out of sand bars by the arrival of the dam-break wave.
- The second assumes that sand bars are substantial enough to remain in place despite heavy erosion by failure discharge.

The first scenario supports evacuation of the dam-break wave and minimizes flood levels. The second forecasts higher flood levels and longer time for flow to return to normal.

Flood levels, according to both scenarios, calculated 500 m upstream from the sand bars, are represented in fig. 6.

Extension of the forecasted estuary flood zone relies in great part on the hypothesis surrounding sand bar resistance. This example refers to failure of minor structures with low-capacity reservoirs. Despite these facts, the example highlights a nearly 3 m vertical difference in peak flood levels even though

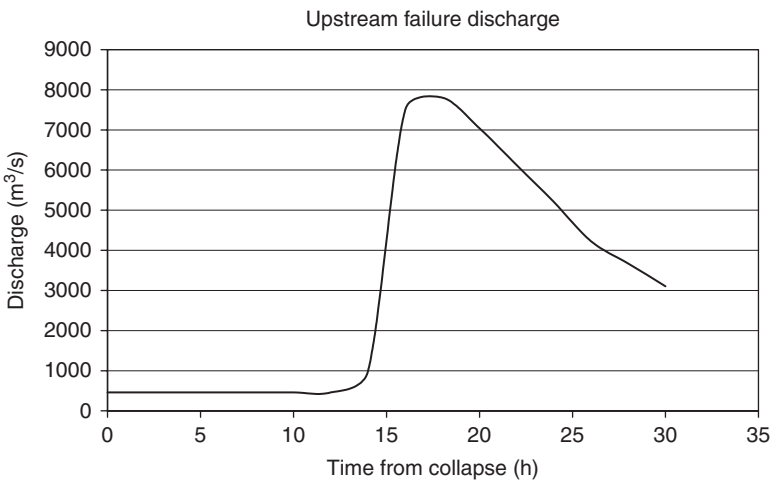

Figure 5: Discharge failure entering the estuary.

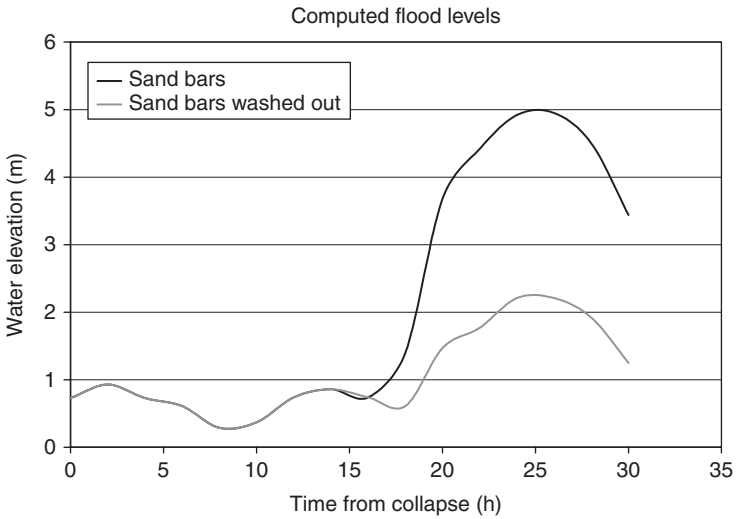

Figure 6: Comparison of expected estuary flood levels according to chosen scenarios.

the dam-beak wave is already significantly attenuated by the river's headwaters. This is not always the case and sand bars are sometimes subjected to progressive but intense erosion during extensive periods of outflow.

4 The problem of debris

Throughout the year, accumulation of debris at certain dams generates maintenance issues and significant operating costs. Debris is also a major factor in the risk of malfunction and failure of a facility. The behaviour of debris must always be taken into account in safety studies (CDA, [10]).

4.1 Composition of debris

The composition of debris and its behaviour vary widely depending on topographical, geological and climatic characteristics of the river's watershed and high-flow channel.

Mountainous watersheds are known for the frequent release of torrential activity and mudflows of highly heterogeneous granular material. The rheological behaviour of these flows depends largely on the content of fine fraction. Most of them contain more than 10% of fine particles smaller than 40 μm and are referred to as muddy debris (Laigle, [11]). In simple shear conditions, the behaviour of such muddy debris flow is non-Newtonian and well described by a Hershel–Bulkley model expressed by the equation:

$$\tau = \tau_c + K(\mathrm{d}u / \mathrm{d}y)^n \tag{2}$$

in which τ_c is the yield stress and K a flowing coefficient. According to the work of O'Brien and Julien [12], K and n are directly linked to the concentration of solids in the mudflow, and according to Coussot [13], n is approximately 0.33.

Predicting the failure of unstable or newly formed deposits hinges on understanding their rheological properties. This knowledge also enables more accurate simulations of the propagation of mudflows containing large amounts of debris by factoring in the additional energy expended by the mudflow and introducing additional friction term S_i in the formulation of the conservation of the quantity of motion in St. Venant equations (Fread, [14]).

At lower altitudes, forest watersheds are subject to uprooting as well as transport of large quantities of trees and other wood debris left behind by fires or logging. There is no reliable procedure to estimate the quantity of debris that may be generated in a given location along a river, except to compile the quantities that are regularly removed from the trash racks of existing structures. Failing such an experience, an accumulation based on an area equivalent to one or two percent of flooded woodland may be adopted.

Finally, in the most urbanized zones, floods that exceed the 20- or 100-year recurrence rate severely damage waterfront development. Floodwaters lift and carry away wharves, vehicles, walls and other construction items, concentrating them at the first contractions encountered along the way.

4.2 Debris blockage

When discharge is heavy or during floods, water carries large quantities of various solids, sometimes over great distances. While debris concentration in the water increases downstream, flow transport capacity diminishes through certain ineffectual sections of the riverbed. The combination of these two trends can create significant, rapid localized blockages. Such blockages were frequently observed during exceptional natural floods at evacuation structures of river dams. Studies were also carried out in a number of specific situations (Braudick, Grant [15]).

The event observed at the Palagnedra Dam (Switzerland) illustrates this danger well (Comité français des barrages, [16]). The 72-m arch-gravity dam retains 5 million m^3 of water and is comprised of a 13-bay free-crest spillway, the pillars of which support a road bridge. In August 1978, heavy rains resulted in a 1500 m^3/s flood wave, which was more than three times the dam's design flood. The water deposited approximately 1.8 million m^3 of sand and gravel in the reservoir. More than 25,000 m^3 of trees and various woody debris partially obstructed the bay gates. Overtopping and erosion of a 30-m high and 25-m wide breach in the right-hand support helped avoid a failure of the dam itself. A similar situation was observed at the Chute Garneau Dam on the Chicoutimi River (Canada) in 1996 which resulted in circumvention of the spillway (fig. 7).

Occasional movement of debris is known to be dangerous because it rapidly and significantly reduces the structure's spillway capacity. It is also considered dangerous because of resulting difficulties in all areas of production and control.

In a report issued in 1999, the National Performance of Dams Program at Stanford University studied the role of debris in 59 dam events, most of them reported after 1990. Debris was the major cause of failure observed in 14 of these cases. Table 1 shows the various effects and their relative importance.

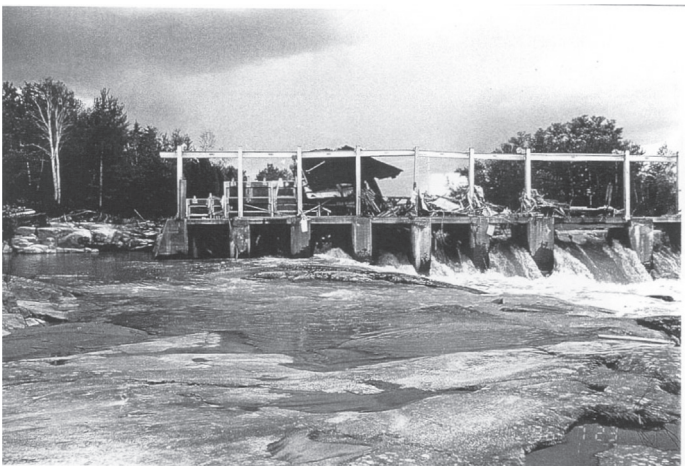

Figure 7: Debris blocking the Chute Garneau dam.

Table 1: Effect of debris accumulation at 59 dams studied in the USA (FEMA, [17]).

Effect	%
Plugged conduit or riser	39
Plugged spillway	30
Damage to or blockage of gates	14
Contribution to scour or impact load	7
Plugged trash racks	5
Damage to trash racks	3
Debris boom cable failure	2

The events studied also reveal that small dams are more susceptible to debris, and operators of small dams are often less prepared to receive debris and react to its presence.

Swedish guidelines on design flood have led to a review of spillway capacity. In a recent research project, Vattenfall's Research Laboratory studied the probability of trees passing a spillway opening and the reduction in spillway capacity due to debris (Johansson and Cederstrom, [18]). The determining factor appears to be the ratio between length of debris L and width of the bays B. Blockage begins when the L/B ratio approaches 2. As for reduction in spillway capacity, it seems to depend entirely on the aspect of opening ratio H/B.

4.3 Loading caused by debris

Debris is also the cause of increased loading on bridges and storage reservoirs (Diehl, [19]). Kennedy [20] describes the mechanism by which pulpwood is acting on a boom, and Michel [21] evaluates similar action exerted by floating ice. These models are useful to estimate the horizontal additional force generated by debris on a dam. This force is given by the summation of the wind friction drag (FA) and the water friction drag (FW) on the length of the debris accumulation (NVE, [22]; (eqn. (3)).

$$\mathrm{FR} = \mathrm{FA} + \mathrm{FW} \tag{3}$$

Research at the Norwegian Water Resources and Energy Directorate (NVE) shows that the leading term is always FW, which can be estimated by eqn. (4)

$$\mathrm{FR} = F_\mathrm{w} = C_\mathrm{d} B_\mathrm{d} (30 T_\mathrm{s} + L_\mathrm{d}) \rho_\mathrm{w} \tag{4}$$

where: F_w is the total force exerted by the debris; C_d a variable coefficient varying between 0.06 and 0.1 depending on v/v_s; $v/v_\mathrm{s} < 1$, $C_\mathrm{d} = 0.06$; $v/v_\mathrm{s} > 1$, $C_\mathrm{d} = 0.10$; v the average velocity of water upstream from debris zone; v_s the average velocity of water under debris; B_d the width of accumulated debris; T_s the immersed depth of debris; L_d the length of accumulated debris and ρ_w the water density.

More recently, a theoretical analysis and several flume tests have been conducted at National Taiwan University to study the mechanism involved in an impact process of debris flow. A complete formulation of the total force has been developed. Experimental and theoretical results show that this impact force is low on dams compared to the other effects of the static pressure of the flow, the weight of the debris volume, the shear stress and the dynamic pressure (Liu *et al.*, [23]).

4.4 Debris and the dam-break wave

Factoring in debris when conducting safety studies means first determining the maximum load each structure can bear. The water surface elevation that will cause a structure to fail corresponds to its maximum hydrostatic load minus the potential resultant load of debris FR. The result is a possible change in the estimated time of the failure and the maximum flood times determined for downstream areas.

However, the resulting additional flow resistance can also cause debris jams in specific zones along the valley and sometimes occurs during natural flooding (Dudley *et al.*, [24]). These temporary retentions are highly unstable, especially when they contain soil and ice as in mountains. They can store large quantities of water and suddenly release it after a few hours or a few days, before controlled draining can be carried out. These retentions contribute to an increased risk of failure and simulation implies taking into account plausible scenarios.

In order to carry out a reliable analysis of the safety of reservoirs established along a watercourse, it is necessary to assess the quantity and level of instability of the debris potentially released by the watershed. Therefore, the effects of each type of debris on flow as well as on dams and control structures must be factored in independently or together. Finally, estimates of the probability of a debris jam and its eventual release after a certain time must be computed. Each situation becomes a specific case for which it is vital to assess specific potential dangers.

5 Influence of ice

In northern regions, thrust applied by ice is one of the most important forces in the design of a hydraulic structure. Ice action against the structure is at least of four types: static pressure due to thermal expansion or contraction, impact of moving ice sheets, pressure from ice accumulation and vertical forces due to variation in water level. All these effects are discussed by Michel ([25]) considering normal operation of the structure.

In the majority of dam safety studies, even those conducted in northern countries, forecasting of dam-break wave propagation is carried out without considering winter conditions. Yet, it is obvious that in such a situation, the dynamic and vertical forces exerted against the ice cover may rapidly prevail and modify the estimated consequences on downstream structures. In light of this, what could be changed by ice and ice covers on the propagation and on the consequences of a dam-break wave coming from upstream?

Several methods and 1D or 2D software have been developed, with satisfactory results, to determine flow conditions during dam failures. These methods are limited, however, because they analyse the dam-break wave propagation under free-surface conditions only; furthermore, no methods have been developed to deal with partially ice-covered rivers or channels where free surface and pressurized conditions may exist simultaneously.

Some experimental work has been carried out recently to propose a methodology to model flood wave propagation in partially covered channels (Fuamba *et al.*, [26]). A numerical model is proposed to track wave propagation in the channel and predict the loadings acting on the cover and the upstream face of the next dam. These loadings are then used to evaluate the structural response of the ice-dam structure.

Dam-break wave propagation is tracked using a numerical formulation where the flood wave is divided into two components: (i) the free-surface sub-wave propagating over the cover, and (ii) the pressure sub-wave propagating under the cover with the water hammer celerity. The formulation implements the numerical MacCormack and water hammer schemes to predict the hydrodynamic flow conditions in free surface and pressurized zones, respectively. While propagating in the channel, the flood wave applies uplifting pressure on the cover and hydrodynamic thrust on the dam downstream.

In order to predict these loadings, the numerical model developed by Fuamba *et al.* [27] simulates unsteady flows in partially covered channels under the following assumptions: (i) the channel bed and lateral sides are rigid; (ii) no sediment transport

is considered; (iii) initial flow conditions are indicated by a steady flow and (iv) the channel cover is rigidly attached to the river banks and the upstream dam face.

As observed during experimental studies, the water flow zone between two consecutive dams can be subdivided into zones I, II and III, shown in fig. 8.

In fact, this work was initiated to investigate dam-break waves caused by failure of hydroelectric dams built in cascade. More specifically, the case study tested in the lab is inspired by the analysis of real rivers such as the one illustrated in fig. 9. The map shows two approximately horizontal segments of the Ottawa River

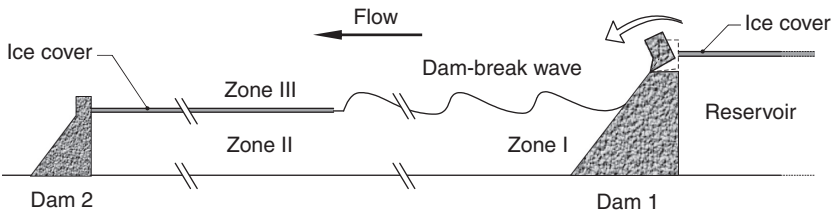

Figure 8: Flood wave propagation zones.

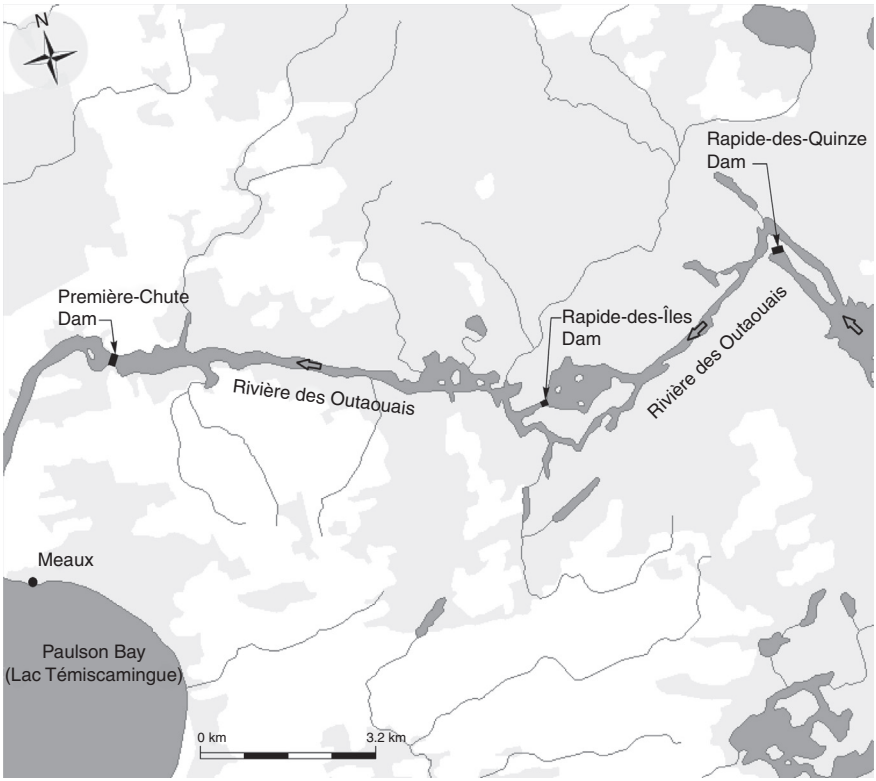

Figure 9: Dams built in cascade on the Ottawa River, Quebec (Canada).

(Quebec): (i) the first section delimited by the Rapide-des-Quinze Dam upstream and the Rapides-des-Îles Dam downstream, and (ii) the second section delimited by the Rapides-des-Îles Dam upstream and the Première-Chute Dam downstream. In winter, it has been observed that water flows under free-surface conditions only in a small fraction of the two river segments described above. The flow continues on a longer path of approximately 5 km, under an approximately 1-m thick ice cover, and through a narrow section with an average width of about 200 m.

5.1 Hydraulic considerations

These conditions justify the assumption of a pressurized flow under a rigid ice cover and the rigid boundary conditions adopted in this work. Indeed, due to the relative proximity of the two consecutive dams, a violent failure of the Rapide-des-Quinze Dam would generate a steep front flood wave extending straight across the two river segments without attenuation before reaching the ice cover. This initial condition is more severe than that corresponding to an ice jam release in large rivers. In the latter case, the breaking front might stop after 'ploughing' through intact ice. It may then resume its motion after a brief rest, or remain stationary and become the toe of a new jam (Beltaos, [28]).

Once the flood wave is created, it starts propagating into zone I as an unsteady free-surface flow until it reaches the cover. At the covered channel entrance, the flood wave divides into two sub-waves: (i) a pressure wave propagating within zone II under the cover, and (ii) a free-surface wave flowing within zone III over the cover. To predict the dam-break wave propagation, the numerical formulation simulates unsteady flow conditions through each zone. The appropriate governing flow equations and numerical solvers have been selected to take into account the free-surface wave propagation, the cover entrance condition and the pressurized wave propagation.

As long as the channel cover remains attached to the riverbanks, wave propagation is followed by an increase of pressure gradient to accommodate the increased discharge. The uplift pressures will exert a hydrodynamic load on the cover, causing crack formation when maximum tension or compression strength of the cover is exceeded. The cover and the downstream dam have been modelled using finite elements to investigate their dynamic structural response under hydrodynamic pressure. It was assumed that the cover is clamped to the channel lateral walls and to the downstream dam, and that its upstream edge is free. The results of the finite element analysis are used to validate the assumption of a rigid cover.

The numerical formulation developed has been applied to a physical model tested in a hydraulics laboratory. The longitudinal cross-section of the experimental set-up is illustrated in fig. 10. The tested model consists of:

- a 6.55-m long, 0.38-m wide and 0.61-m deep rectangular and horizontal channel;
- an upstream reservoir with one lateral face that is a 0.40-m long weir. The upper part of the weir is 0.105 m high and located over the door which is used to create flood waves;
- a 0.38-m wide and 0.22-m high downstream dam provided with a gate;

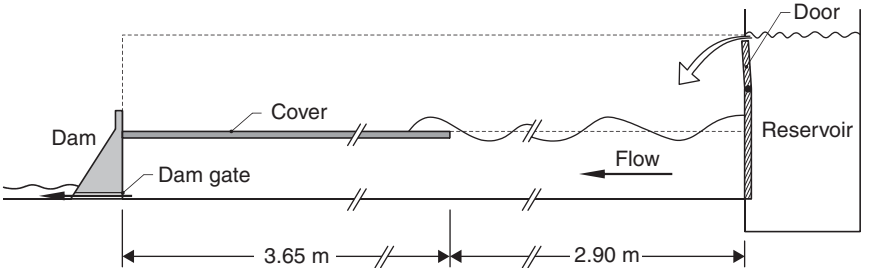

Figure 10: Longitudinal cross-section of the experimental set-up.

- a 3.65-m long and 0.019-m thick cover, fixed at an elevation of 0.17 m from the invert.

It should be mentioned that although the horizontal rectangular shape used is not necessarily that of a real channel, this simplified geometry is adopted to focus on the feasibility of the mixed numerical model proposed.

The Manning coefficient values calibrated using the numerical model are 0.002 in the free-surface zone which corresponds to zone I in fig. 8, and 0.005 in the covered zone which corresponds to zone III in the same figure. In the pressurized zone II, the mean calibrated value of the Darcy–Weisbach coefficient for the representative case study is 0.021. The downstream boundary condition is set by a valve. Water levels and pressure measurements were taken in zones I and III and in the vicinity of the downstream dam heel in zone II.

The experimental results have been compared with the numerically predicted ones. Initial flow was a permanent discharge. An upper-boundary compression wave celerity $c = 1480$ m/s within the covered part of the channel was used in this study. Twelve laboratory tests were conducted using the horizontal rectangular channel. The same trends were observed in all the tests. Figure 11 shows the comparison between typical measured water depths and those predicted by the model at the downstream dam. The predicted incident flood wave amplitude is similar to the measurements (27.6 cm vs. 27.4 cm).

The hydrodynamic conditions in the partially covered channel have been verified. Figure 12 shows the comparison between the pressure head predicted and the recorded values under the cover at the downstream dam section. The pressure wave arrival time and amplitude are quite similar between prediction and measurements.

It may be noted from figs. 11 and 12 that oscillations observed on measurement values are not reproduced by the numerical model. This is because the St. Venant equation for the free-surface propagation and the equation for the pressure wave propagation always stop the secondary oscillations. By using the Boussinesq equations with the secondary derivative, one can restore these oscillations, which have negligible physical impact on the dam loading.

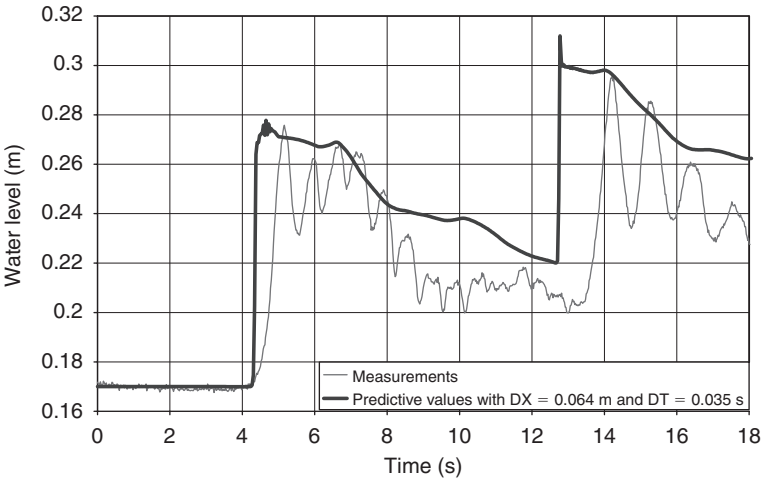

Figure 11: Comparison between measured and predicted waterdepth values at the downstream dam.

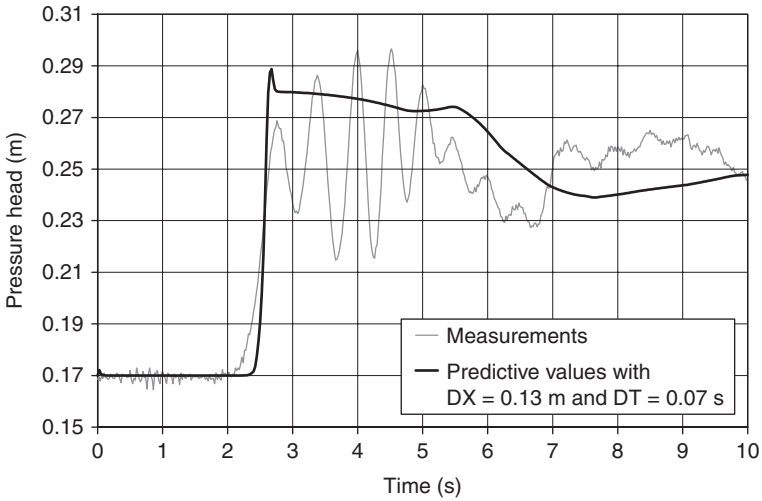

Figure 12: Comparison between measured and predicted pressure head values at the downstream dam in zone II.

5.2 Ice cover mechanics

The numerical model helps to figure out the free surface and pressure wave propagation along the channel and to predict the cover and the downstream dam loading. As mentioned previously, the channel cover is assumed to be clamped

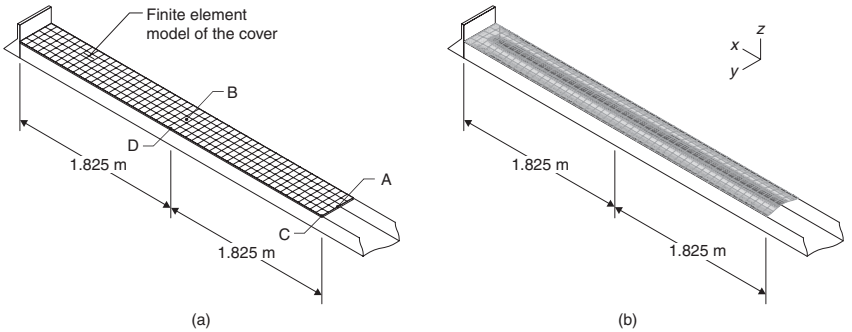

Figure 13: Structural response of the cover: (a) finite element model, (b) deflection and stress band plots of the cover subjected to uplifting hydrodynamic pressures.

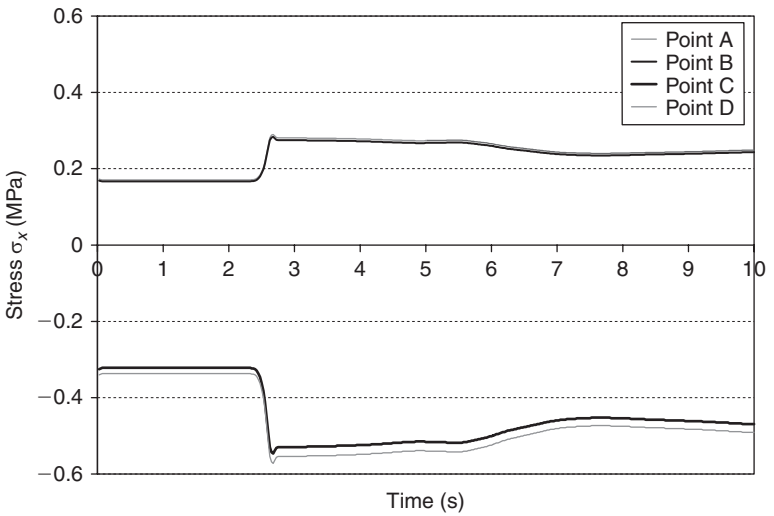

Figure 14: Normal stresses σ_x calculated at the cover upper surface.

to the channel walls and to the dam upstream face. In a second step, a finite element model of the ice cover was built using 16-node shell elements, as shown in fig. 13(a). The hydrodynamic pressure load obtained from the hydraulic analysis described above has been applied to the cover as a dynamic uplifting distributed force. The stresses and the deflections permeating the entire ice cover are determined. For the purposes of illustration, fig. 13(b) shows band plots of normal stresses σ_x obtained at the cover surface.

For a closer look at the structural response of the cover, normal stresses σ_x at points A, B, C and D located at the upper surface of the cover are shown in fig. 14.

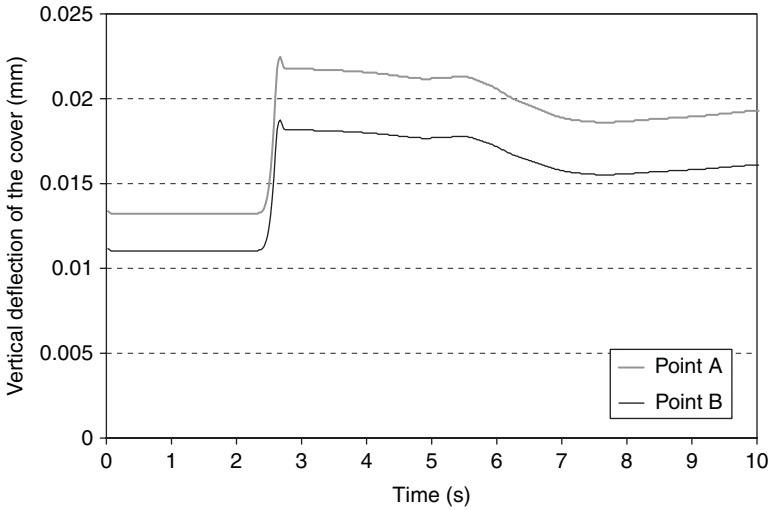

Figure 15: Vertical deflections at the cover upper surface.

Normal stress variations follow the same trend as water depth values predicted at the dam upstream face (fig. 11). As expected, the upper surface of the cover is under compression along the channel lateral boundaries, and under tension along the longitudinal middle axis of the cover. The occurrences of maximum compression and tension stresses correspond to the peak predicted water depth. It is important to note that the stresses after flood wave arrival are sustained at approximately constant values as the pressure wave propagates under the cover.

The vertical deflections permeating the cover are also obtained using the finite element model. As illustrated in fig. 15, not only the deflections at points A and B follow the same trend as the hydrodynamic loading, but the maximum predicted deflections are also lower than the predicted value. This clearly indicates the extreme rigidity of the cover. This result validates the assumption of an acoustic wave celerity corresponding to a rigid cover. The rigid cover is used to verify the stability of the numerical schemes used. Although these findings apply strictly to the experimental set-up described above, some extrapolations have been made to understand the behaviour of real ice covers under dam-break wave effects.

5.3 Dam response

Assessing the structural response of the downstream dam under flood wave hydrodynamic loading is of utmost importance. Figures 16 and 17 show deformed finite element meshes of the dam with and without the ice cover, respectively. The dam is subjected to the hydrodynamic loads obtained from the hydraulic analysis of the free surface or covered channel described above.

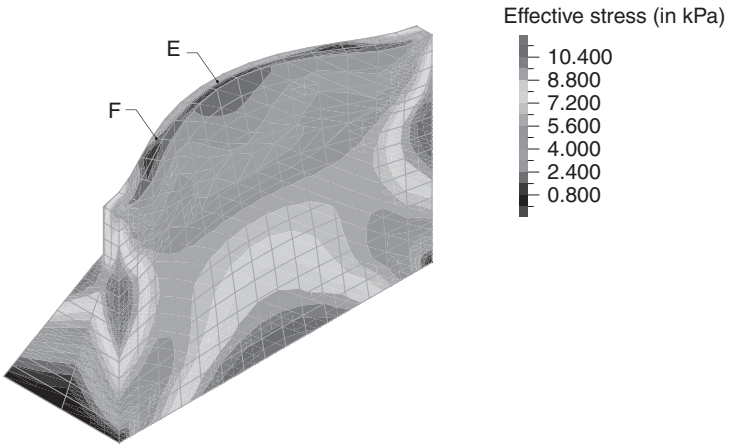

Figure 16: Effective stresses on the dam without ice cover.

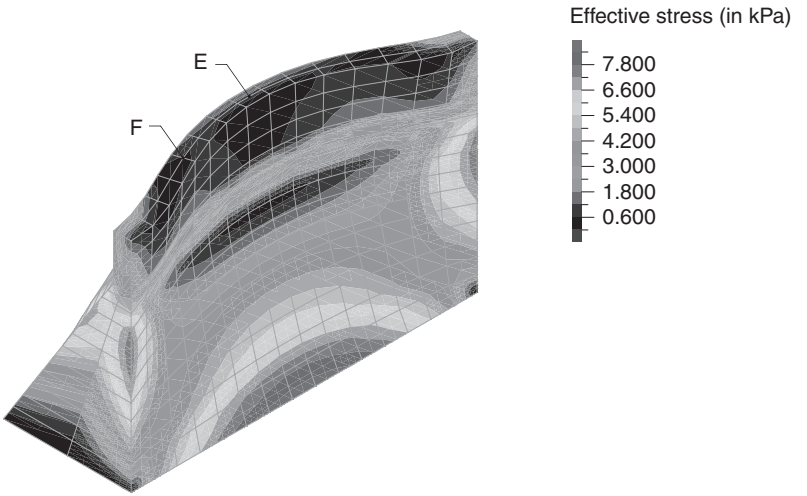

Figure 17: Effective stresses on the dam with ice cover.

Overall, the resulting stresses on the dam decrease when the effect of the cover is included in the analysis. Furthermore, the dam lateral deflections become smaller when the channel is covered. This rigid structural behaviour, also observed for dams subjected to forced-vibration loading (Bouaanani *et al.* [29]), should be interpreted with the following precaution: the foregoing results assume that the ice cover is rigidly connected to the dam upstream face, thus restraining the upstream–downstream displacements, but in real situations the dam-cover connection is more complex, and excessive cracking can cause the

cover to detach completely from the dam face under high loading. It should be noted, however, that the hydrodynamic load would be higher due to the presence of the cover, even in the case of complete detachment.

Numerous studies are still required to better understand the effects of ice on dam-break waves in a multi-dam hydrological system. The small amount of available concrete knowledge on the topic and the complexity of applicable numerical treatments undoubtedly explain why winter failure scenarios are not required by regulatory authorities, even in countries where ice covers are common and present for 4–5 months.

6 The presence of a downstream dam

In order to effectively harness the full hydraulic potential of certain rivers, the most commonly used development scheme is comprised of several dams built in cascade on the riverbed. Each structure constitutes an obstacle for upstream dam-break wave propagation and may increase or decrease the flood's impact.

Safety studies of such a hydraulics facility involve multiple scenarios in which a dam-break wave quickly reaches a structure located immediately downstream, overloads the structure, fills the reservoir and potentially causes its failure. The result is a succession of overloads and failures or uncontrolled spills, the evolution of which depends on the multiple characteristics of the structures involved in the event (available storage, spillway capacity, reaction time, probability of safe spill-over, etc.) as well as on the human or automated responses within the system.

1D and 2D numerical models based on dynamic equations are able to rapidly and appropriately manage the flow dynamics. Older calculation codes divided the river into successive reaches. For each calculation, the downstream dam was used to define downstream boundary elevation conditions, which were then used to regenerate flow variation with time upstream from the second reach and so on.

Current numerical models include conditions referred to as internal and their role is to represent flow behaviour in areas where St. Venant equations cannot be applied. For example, in the downstream section of a dam, elevation is dictated by flow and the structure's spillway characteristics while outflow is transferred downstream from the structure and becomes an upstream condition for the following reach. Various components of the dam may be taken into account, including gates, spillways, turbines and breach formation. This type of calculation allows systematic tracking of the various phases of dam-break wave flow. It offers the possibility of opening the local spillway and anticipating the arrival of the dam-break wave by simulating preventive spillage of the downstream reservoir.

However, the dynamic behaviour of the hydrological system depends much more on resistance or failure of the obstacle structure. For structures known as rigid

(concrete arch, gravity dam and rolled concrete dams mainly) the same approach also allows factoring of actual resistance or estimated resistance of the structure to slipping and overtopping. In northern countries, for example, stability of a rigid structure is not called into question until water spilling over the top exceeds 1 m, because excess water pressure does not exceed the outward force of ice factored into the design of the structure.

This may be extended to compliant structures (earth, rockfill, upstream facing etc.) to factor in assumed resistance to spill-over and progressive erosion. However, other methods of tracking actual behaviour are now available for certain simple earth and rockfill structures. They are identical to those discussed in part 9 on road embankments.

Results obtained with regard to the flow of an upstream dam-break wave in a cascade may seem surprising. The following example relates to the successive failure of two facilities, where the reservoir elevation of the downstream structure, an earth and rockfill dam, is maintained at maximum level at all times. Figure 18 first shows the hydrogram of the initial flood wave, which began more than 60 km upstream, as it flows into the reservoir of the obstacle structure. Increase in flow discharge appears fairly regular. The second curve represents the flow rate downstream from the obstacle structure and is calculated based on the assumption that the structure cannot resist overtopping in excess of 1.0 m. The local peak presented by the second curve is a result of this behaviour hypothesis and a chosen failure time of 0.5 h. Downstream flow rate is slow to increase then rapidly increases to an initial peak before decreasing during a fraction of time, then increasing again, and levelling off. A detailed study of the first curve reveals a

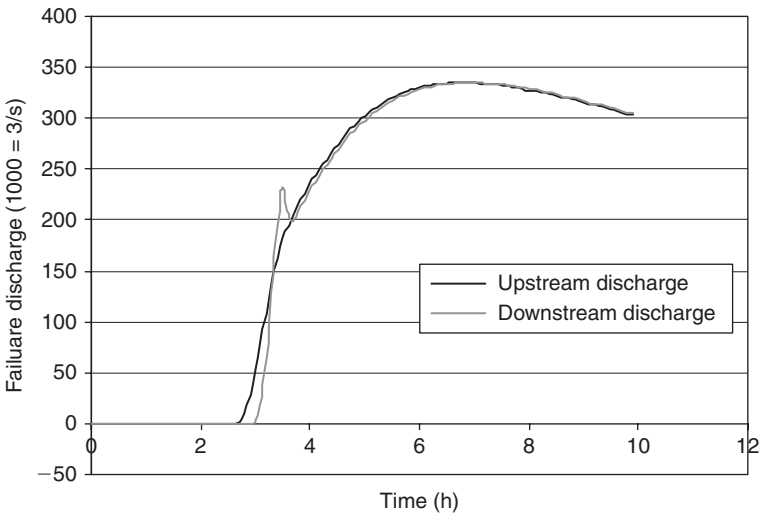

Figure 18: Hydrograms calculated on either side of the obstacle dam.

change in the rate of change of the upstream hydrogram at that moment. Evolution of elevations on either side of the structure reveals a situation that is specific to the characteristics of this facility.

Upstream, the arrival of the initial dam-break wave front causes an increase in the elevation of the downstream reservoir to the level of failure by overtopping. Breach formation in the obstacle structure slows the rise, thus allowing stabilization and partial spill-over of the reservoir. However, arrival of the bulk of the water from the upstream failure, greater than the capacity of the breach, causes the reservoir to fill up again beyond its initial level of operation. Downstream from the obstacle structure, initial filling of the reservoir and overtopping slowed the water's rate of rise for a while. Then, spill-over of the reservoir downstream from the dam-break failure accentuates submerging which decreases after approximately a quarter of an hour before increasing again under the influence of the principal failure (fig. 19).

Due to the form of the equations used and the hypotheses stated (specifically hydrostatic pressure), the resulting solutions present certain limitations and do not always reflect the actual complexity of the flow. In certain sequences, a negative wave moves through the downstream reservoir and presents secondary oscillations that current numerical methods cannot factor in. The result is an illusion of stability in calculated elevations that is well illustrated in physical model tests. However, these inaccuracies, which are most often observed in the initial moments following the arrival of the dam-break wave front, have little impact on estimation of the flood mark, or alert and reaction times calculated to meet the requirements of emergency measures plans.

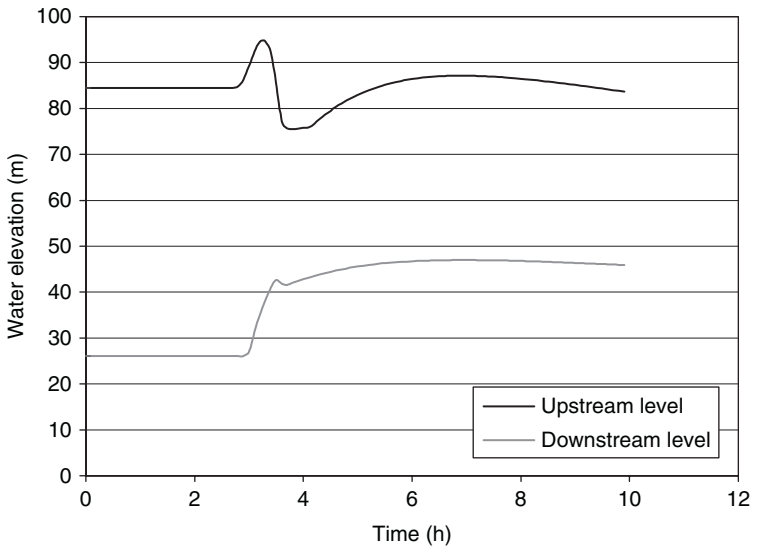

Figure 19: Limnographs calculated on either side of the obstacle dam.

7 Presence of a bridge on the river

In permanent and non-permanent regimens, a bridge usually inhibits flow and constitutes a significant obstacle to the passage of floods and dam-break waves. Abutments and piers produce a localized restriction of the low-flow channel, which builds as flow increases and becomes significant as the river reaches its flood level.

Upon arrival of the dam-break wave front, a partial positive reflection of the wave moves upstream and depending on the slope of the river, it may affect the local flow regimen and the position of a possible hydraulic jump. However, the scale of dam-break waves is often greater than that of the natural floods used to determine the position of the bridge deck. In light of this, two aspects must be factored in.

The first is blockage by floating debris (trees, wharves, boats, etc.) carried by water in the floodplain. When water surface elevation reaches 0.20 m from the bridge deck, the deck acts as a boom and retains part of the debris upstream. The presence of this cover, the area of which rapidly increases on contact with the water, increases local head loss. Water deceleration translates into a greater rise in upstream elevations. For a few moments, the bridge acts as a local retainer of water and debris and translates into increased horizontal pressure on the bridge deck.

However, in order to allow expansion and contraction due to changes in temperature, bridge decks are often set on single supports. Under the combined effects of buoyancy from the water as it is immersed and the horizontal thrust from the debris, the deck may slip off its supports and fall into the riverbed, as shown in fig. 20. This fall frees the temporarily formed reservoir and part of the accumulated debris resulting in a temporary increase in the rate of rise downstream.

In accordance with the capabilities of current calculation models, the user may factor in the presence of bridges in many ways.

1. The first and simplest is to factor in the direct impact of a bridge in the path of a dam-beak wave as you would a cross-section restricted locally to the available width, regardless of elevation. Local head loss may be assigned to the section in order to factor in the effects of contraction and expansion on the flow. Therefore, there is total elimination of the bridge deck once the water has reached it and the role of potential debris can be ignored as well as the possible erosion of abutments or part of the approach fill.
2. The second possible method was proposed by Fread [14]. It consists in assuming that the bridge deck will remain in place during the flood and defining an internal boundary condition for the bridge section. This condition can be expressed as follows:

$$Q_i = Q_1 + Q_2 = Q_{i+1} \tag{5}$$

Figure 20: La Baie bridge after the failure of the Ha! Ha! dam.

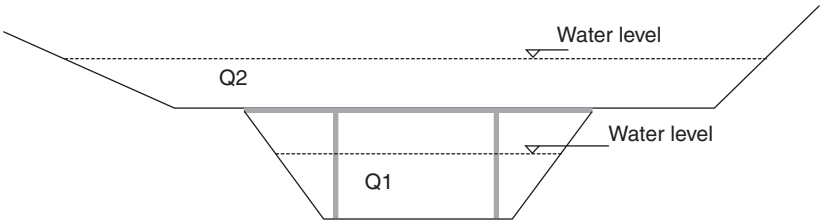

Figure 21: Model section of a bridge according to Fread [14].

Discharge Q_i in eqn. (5) is the sum of discharges flowing through different parts of the bridge flow area. When the water flows normally under the bridge deck (see fig. 21), the base flow is given by the usual formula (eqn. (6)):

$$Q_1 = CA(2g\Delta H) \tag{6}$$

in which

- C is a discharge coefficient which factors in the presence and shape of pillars and abutments;
- A is the flow area at the downstream boundary of the bridge;
- ΔH is the variation in hydraulic load at the bridge.

When the water-level elevation reaches the bridge deck, flow through the bridge opening is considered under pressure and coefficient C is modified accordingly. Finally, when water passes over the bridge and approach fills, we must add Q_2, the contribution from lateral wall overtopping. In all cases, downstream submergence must be assessed in order to adjust the flow coefficients of all contributing parts. Flow is transferred entirely to the downstream section.

Moreover, at this level an additional increase in capacity can be introduced to represent breach formation in the approach fill, in accordance with the proposed procedure to factor in erosion or internal erosion of embankments.

3. Finally, it is possible to introduce flow resistance control rules or variation of the actual flow section to this calculation as a function of time, discharge or calculated instantaneous elevation. The FIREBIRD and ERODE prediction codes developed by the École Polytechnique de Montréal offer this possibility (Marche, [4]). However, these codes draw on newly available information relating to debris flow and are more suited to current dam safety research than common practice.

8 Presence of an embankment with or without a culvert

In order to accommodate road or rail crossings or to protect flood zones, the course of certain rivers is constrained by embankments. When there is a drain or culvert in these embankments, its diameter is generally small compared to the height or width of the embankment. The arrival of a dam-break wave at the embankment generates a change in dynamic flood behaviour that is similar to the behaviour observed upstream from a dam. However, several major differences must be considered in order to predict resulting events:

a) the volume of the potential reservoir upstream from the embankment is generally low;
b) if the embankment includes a culvert, the culvert's capacity is low compared to the inflow of water from the failure and
c) the embankment, which was not designed as a dam, will rapidly become saturated during loading and will exhibit low resistance to erosion.

The result is a specific flow dynamic, which displays an initial increase in water flow downstream, followed by low discharge stabilization. Meanwhile, the increase in upstream inflow generates a rapid rise in elevation at the embankment and causes loading of the culvert. High interstitial pressure develops at the embankment around the culvert and may increase the risk of internal erosion of the structure from that moment. However, the upstream elevation quickly reaches the crest of the embankment and results in surface overtopping over a progressively greater distance. From that moment, a heavy increase in overtopping

capacity is possible. This occurrence means that upstream water elevation will be only slightly increased and upstream level stabilization may be observed. The crest of the embankment will undergo high shear stress and erosion will begin and intensify. The breach or breaches formed in the embankment, associated with the possible extraction of the conduit under the effects of internal erosion, result in breaching in part of the natural riverbed.

A common variant of this dynamic is observed when water rises rapidly upstream from the embankment or embankment resistance is abnormally high. This leads to overflowing riverbanks and circumvention of the embankment through a breach in one of the riverbanks, which are less resistant than the structure itself. In certain topographies, this may result in complete displacement of the riverbed.

Processes involved in this dynamic (blockage by debris, surface erosion, soil saturation, internal erosion, etc.) are quite random as are the state and potential mechanical behaviours of the embankment in case of upstream failure. Predictions of the way a flood wave will pass an embankment and the elevations and flow rates on either side of the structure are often carried out based on a preset embankment behaviour scenario. Flow rise is achieved by simulating pressure build-up on the culvert while ignoring the role of potential debris, for example.

The most common approach consists of introducing an internal boundary condition upon the embankment dictating the discharge in the section, the discharge being equal to the sum of the discharge through an aperture representing the loaded culvert and the spillway discharge representing the culvert running free and embankment overtopping. Results of this calculation depend largely on the choice of discharge coefficients.

A method introduced by Cunge [30] represents the closed flow area of the culvert as a slightly open area at the crest. This method is proposed by Fread in code NWS–FLDWAV, which more accurately represents the flow dynamic and downstream control methods because it does not artificially section the riverbed through an internal condition. However, the width of the aperture must be calibrated to accurately represent wave propagation velocity.

Peak elevations, both upstream and downstream from the embankment, depend largely on the type of embankment failure. Some of the more recent research has led to more accurate predictions of probable evolution. Derived from laboratory trials as well as trials on full-scale structures, recent knowledge has led to a better understanding of how an embankment will fail, the mechanisms that will affect it and how long it takes to fail (Singh, [31];Visser, [32], Wurbs, [33]).

As part of the IMPACT project [34], several experimental dikes were built downstream from the Røssvatn Dam in Norway with the specific goal of testing dam failure by overtopping. Røssvatn Dam supplied and controlled the flow needed to cause failure in the test dikes while the water level was continuously monitored upstream from the embankment. A wealth of additional technical

data was gained from these tests, especially regarding the role of soil cohesion and mechanisms of slope stability in the interaction process of breach formation and on the flood discharge. Figure 22 shows a period of intense deepening and widening of the breach channel by erosion of the thalweg and collapse of the breach sides.

According to our observations (Marche [35]), the first running water seeps (mechanism 1) into the layers of the crest and its overflow simultaneously produces the beginnings of shearing on the surface (mechanism 2). Depending on grain size distribution, initial state of compaction and the evolution of soil water content, resistance to shearing of these layers decreases as shearing action increases. Erosion caused by the detachment of a number of particles (mechanism 3) creates a new flow channel, concentrating factors conducive to shear stress and turbulent flow.

When erosion begins to affect the crest line, it is the onset of breach formation and the rate of breach outflow becomes greater and greater (mechanism 4). All along the new breach channel, banks are formed with a slope dependent on the depth of the thalweg in the embankment. Slope stability is low and reaches borderline levels during gullying. At this point, failure and flow erosion enlarge the breach by successive bursts (mechanism 5) and the same phenomenon occurs in the thalweg of the breach channel (mechanism 6). Not all failures by overtopping involve all six mechanisms but they are a result of a number of them activated by characteristics specific to each case.

Figure 22: View of breach formation.

Breach formation due to crest overtopping is a complex phenomenon in which there is a strong coupling between the flow hydraulics and the changing geometry of the controlling structure. The flow over the crest results in erosion, which in turn modifies the flow behaviour due to the changing geometry of the structure. Modelling this behaviour requires a correct incorporation of this fluid–structure interaction in the formulation. These mechanisms have been deterministically factored into computational codes. ERODE is one of these dynamic simulation tools developed to predict dam failures by overtopping.

From the onset of crest overflow, the evolutions of the discharge and of the embankment are closely linked. The progression of the failure and the creation of an accurate breach outflow hydrograph for each embankment according to foreseen overtopping scenarios can only be done by proceeding systematically using a time-stepping procedure. With ERODE, this prediction is done by successively testing and activating different mechanisms, if need be, as demonstrated in the flow chart presented in fig. 23. The first four mechanisms are well known to hydraulic engineers and certain computational codes address them according to the most current knowledge.

The short versions of ERODE produce a 1D evolution of the water profile and sediment routing induced in the breach channel depending on the flow calculated at

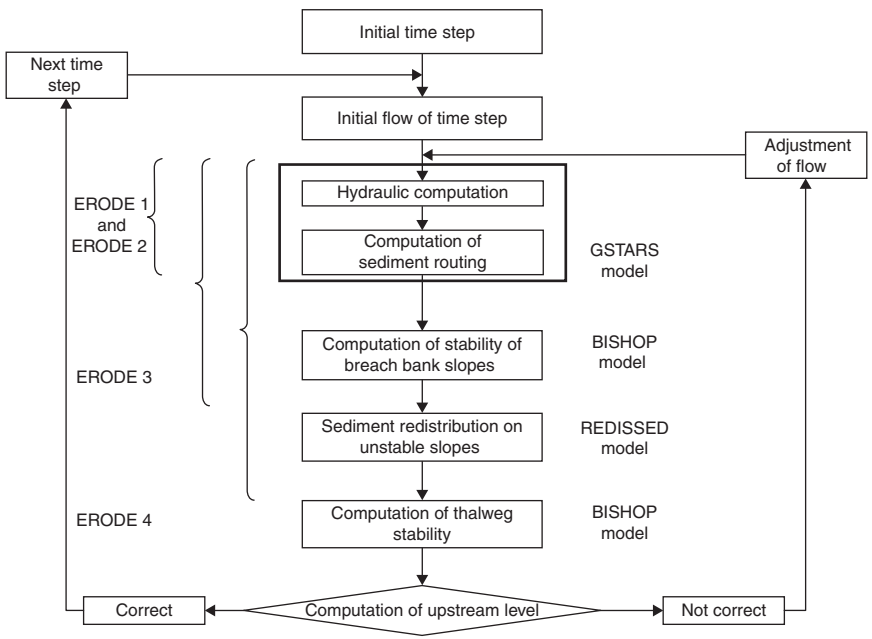

Figure 23: Prediction of dam break and breach flow by ERODE.

each time step. Depending on grain size distribution and cohesion, the best-suited transport function may be selected among six universally recognized sediment transport equations.

- ERODE1 can be used for an embankment with uniform grain size distribution but it is possible to factor in the different layers of an embankment with ERODE2.
- A third version (ERODE3) was developed and factors in the stability of bank and breach slopes. Additional computations stem from analysis of slope stability. However, the most common methods used by geotechnical specialists cannot be applied to breach calculation for several reasons. For example, the trial-and-error method requires that the user enter important elements of the solution (centre of the shear circle in the Bishop model for example). The verification of slope stability of both banks of the breach channel at each time step requires a large number of calculations, so it was automated by looking for an optimal solution, i.e. the failure circle with the lowest local safety factor. The various layers of the embankment are factored in. The simplified Bishop model was adopted and a geometric redistribution of sediment was applied to the time step during which the bank failure is diagnosed. The same method was applied to verify the failure of the longitudinal slope in the thalweg (ERODE4). It allows factoring of headcut instability (Mahdi and Marche, [36]). This being said, it is clear that the breach formation model gives priority to circular failure surfaces and factors each side of the breach at the moment it becomes unstable. A delay factor can be added if need be.

ERODE was used in a number of test situations to evaluate its behaviour. The currently available results of the two large-scale tests done in Norway are presented in Marche [35]. The calculated predictions agree with the observed field test results. They allow for the identification of degradation mechanism triggers and the identification of the true role of certain properties of the embankment such as cohesion or compaction of soil material, for example. However, a number of simulations have demonstrated that inherent variability of certain characteristics may influence the interaction between the embankment and the outflow as well as the rate of degradation.

Ongoing research has already allowed the introduction within the highly deterministic model of the behaviour-based approach presented here, of certain statistical elements or other elements inherent to the nature of the materials used or their ageing. When these factors are considered, the computation of the most probable breach flow hydrograph is slightly different from the previous one illustrated in fig. 24.

Current research also shows that the final shape of the dam failure breach is not the result of a chaotic system (in statistics, a system is said to be chaotic if slight variations produce radically different results), which would hardly be reconcilable with the objectives of dam safety engineers.

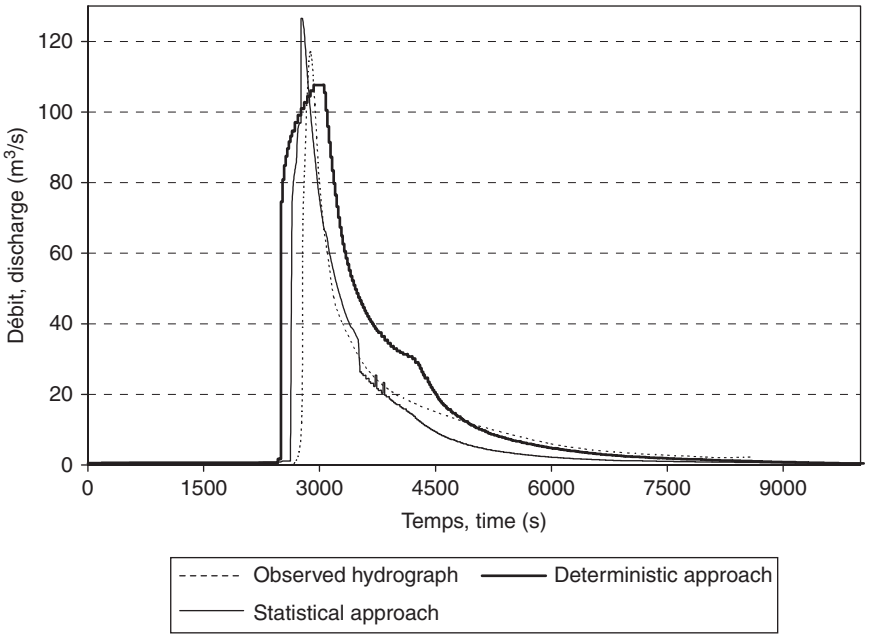

Figure 24: Homogeneous dam without cohesion, breach hydrographs.

9 The presence of an isolated obstacle or a high density of obstacles

Violent floods associated with dam failures can be on such a scale that flooding spreads to uncommon areas generally devoted to other purposes. In such cases, water intersects with roads, embankments and buildings, all of which become significant obstacles to flow. Each of these obstacles profoundly alters flood wave propagation, divides flow and may divert large quantities of water. On the other hand, every obstacle is also impacted in a specific way and presents specific behaviour. Mathematic models commonly used to simulate dam-break flood conditions do not specifically factor in every obstacle. They are factored in mainly because of the increase in the overall flow resistance they produce.

It is well known that factors such as Manning's '*n*' or the Chezy coefficient are not always appropriate to factor in the presence of obstacles emerging from the water. Moreover, when choosing these factors to factor in head loss, it is possible to calculate water surface elevation and local velocity but another step is required to determine potential force on the obstacle, its stability and the possibility of its destruction. The practical significance of such results on dam risk assessment explains the recent multiplication of research efforts in this area.

Between 2003 and 2008, the IMPACT European Group, which aims at investigating dam-break flooding and extreme flooding, carried out numerous laboratory tests and simulations. Among various topics, studies of the behaviour of an

individual obstacle and simulation of the behaviour of a zone with a high density of obstacles have been priority focuses (IMPACT, [34]).

9.1 Isolated obstacle

One of the most significant tests of the series provides a description of how the free surface of the water is affected around a building located at a given angle (64°) to the principle flow axis. Model experiments limit the building's zone of influence, identify the area in which there is a temporary rise in water level and demonstrate progressive reflection against the bank (Noel *et al.*, [37]).

The specialists involved in the experiment used their own 2D model and compared predictions with experimental results. The results showed that upon arrival of the wave, initial rise in water level is identical with or without an obstacle. Later, the presence of the obstacle generates a rapid additional rise corresponding to reflection of the wave. However, downstream, the presence of an obstacle slows the initial rise but subsequent stabilization is similar in both scenarios.

Numerical simulations of various cases produced results very similar to those observed. Calculated evolutions were more stable than those observed and a few problems were encountered locally in the wake of the obstacle. Reasonable errors were observed in the location of the hydraulic jumps and in the reflections on the walls. These results have yet to be transposed in terms of forces applied on the obstacle itself in order to study its stability and durability, for example. However, research in this area is necessary to assess the degree of protection offered by certain large-scale buildings in potential flood zones.

9.2 Groups of obstacles

The second important aspect concerns groups of obstacles. The main question deals with factoring in such a group when it occupies a large part of an inundated area and for which it is impossible to discretize and simulate the effect of each obstacle present. The situation is similar to flood propagation in urban or dense woodland areas, for example. Researchers' current objective is to improve the representation while conserving a realistic level of geometric discretization.

In this case, model experiments were carried out in several laboratories. Figure 25 represents the plan of the study zone dedicated to this specific type of propagation. Figure 26 shows an overall image of the corresponding study model at the Fluid Mechanics Laboratory of the University of Zaragoza (Spain) (Alcrudo *et al.*, [38]).

To simulate local flow properties, it is obvious that a 1D approach is inadequate. Current tests show that various 2D computation methods succeed in generating a credible image of local velocity and depth. However, calculated values appear artificially more stable than those recorded in the laboratory, even when taking into account the fact that model experiments amplify secondary effects. It is possible to adjust the synchronism between maximum observed values and

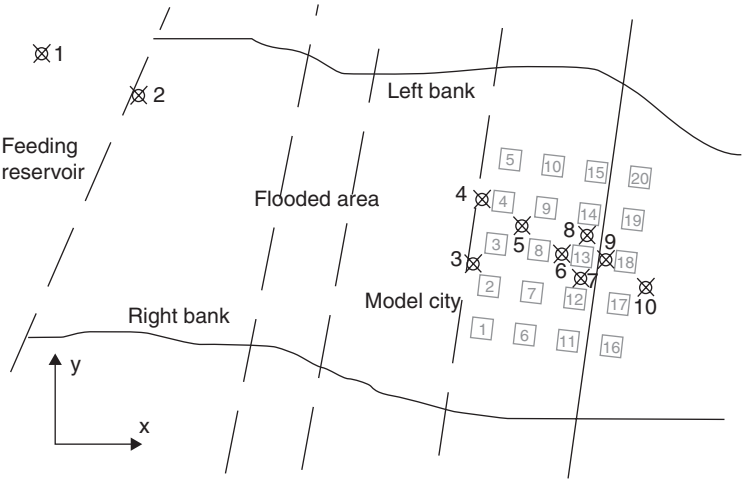

Figure 25: Plan of study zone – groups of obstacles.

Figure 26: Model built for the experiments.

calculated values by fine-tuning the friction term of the surrounding area. From then on, calculated velocities and depths enable estimation of the magnitude of the average dynamic loading on each object. The groups' conclusions are that calculated depths are too homogeneous in the area near each obstacle and the numerical hydrographs are usually underestimated (Murillo *et al.*, [39]).

In order to offset these issues, new simulation techniques have been developed (Ferreira, [40]). The TELEMAC model used at Électricité de France is one example and it resolves 2D shallow-water equations using a finite element analysis (Hervouet *et al*., [41]), the favoured method consisting in introducing a local porosity to represent the local density of buildings, without specifically discretizing every building. This solution applies homogenization through which geometric details are transformed into an ongoing property of the environment. Porosity is added to the mass conservation equation as well as to the dynamic equations. It facilitates a partial reduction of the actual flow surface. Then, local dynamic effects of the obstacles are introduced through the action–reaction equivalence principle.

Tests show that porosity generates and facilitates local acceleration. Upstream from the highly obstacle-dense area, a rise in water level is observed which leads to a greater extension of the inundated area.

Currently available papers show that the presence of aligned obstacles such as buildings or trees may be correctly factored in the resolution of St. Venant equations on the condition that two steps are carried out: adjustment of local porosity in the 2D space being used and adaptation of a friction rule derived from the calculation of drag forces on the obstacles themselves. However, this technique must still be considered as experimental.

References

[1] Anctil, F., Rousselle, J. & Lauzon, N., *Hydrologie, cheminements de l'eau*, Presses Internationales Polytechniques, Montréal, pp. 239–240, 2005 (in French).
[2] Zech, Y. & Spinewine, B., Dam-break induced floods and sediment movement, state of the art and need for research, 1st atelier IMPACT, Wallingford, 2002.
[3] Foda, M.A., Hill, D.F., Deneale, P.L. & Huang, C.M., Fluidization response of sediment bed to rapidly falling water surface. *Journal of Waterway, Port, Coastal and Ocean Engineering, ASCE*, **123** (5), 1997.
[4] Marche, C., *Barrages, crues de rupture et protection civile*, 2nd edition. Presses Internationales Polytechniques, Montréal, pp. 149–159, 2007 (in French).
[5] Singh, V.P. & Li, J., Identification of reservoir floodwave models. Journal of Hydraulic Research, **26** (2), 1993.
[6] Marche, C., Gagnon, J., Quach, T.T., Kahawita, R. & Beauchemin, P., Simulation of dam failure in multidyke reservoirs arranged in cascade. *Journal Hydraulic Engineering*, **123** (11), pp. 950–961, 1997.
[7] Hakin, W.D., Jones, B.A. & Cazaillet, O., Safety measures adopted to increase spillway potential at Jindabyne dam in the snowy mountains. *ICOLD Proceedings*, Barcelona, 2006.
[8] Marche, C., Gagnon, J., Quach, T.T., Les digues fusibles, un élément de sécurité additionnelle dans un aménagement hydroélectrique. *CJCE*, **22** (3), pp. 566–575, 1995.
[9] Hydrocosme Inc., Étude des conséquences possibles de la rupture des barrages CH4 et P2 dans la rivière Moisie, Montréal, 1991.
[10] CDA, Dam safety, Canadian Dam Association, *Technical Bulletin Hydro Technical Considerations for Dam Safety*, pp. 1–49, 2007.

[11] Laigle, D., A two dimensional model for the study of debris-flow spreading on a torrent debris fan, Debris-flow hazards mitigation. *Proceedings of the 1st International Conference, ASCE*, San Francisco, pp. 123–132, 1997.
[12] O'Brien, J.S. & Julien, P., *Physical properties and mechanics of hyper-concentrated sediments flows*. Utah State University, Utah Water Research Laboratory, Logan, Utah, UWRL/G85-03, 1984.
[13] Coussot, P., Steady, laminar flow of concentrated mud suspensions in open channel. *Journal of Hydraulic Research*, **32** (4), 1994.
[14] Fread, D.L., *NWS FLDWAV model, theoretical description*. Hydraulic Research Laboratory, Office of Hydrology, National Weather Service, Silver Spring, Maryland, USA, 1999.
[15] Braudick, C.A. & Grant, G.E., When do logs move in rivers. *Water Resources Research*, **36** (2), pp. 571–583, 2000.
[16] Comité français des barrages, *Practical guidelines for improvement of dam safety during floods*. FRCOLD News, no. 8, ISNN 1256-5202, Le Bourget du lac, France, 1998.
[17] FEMA, Federal guidelines for dams safety, FEMA Distribution Center. *Hydrological Review*, **18** (2), pp. 76–78, 1999.
[18] Johansson, N. & Cederstrom, M., Floating debris and spillways. *Proceedings of the ASCE Conference on Hydropower*, Waterpower'95, San Francisco, pp. 2016–2115, 1995.
[19] Diehl, T.H., *Potential drift accumulation at bridges*. Publication no. FHWA-RD-97-028, US department of transportation, federal Highway administration research and development, Turner Fairbank Highway research Center, Virginia, USA, 1997.
[20] Kennedy, R. J., *Forces involved in pulpwood holding grounds*. Pulp and Paper Research Institute of Canada, 1962.
[21] Michel, B., *Thrust exerted by unconsolidated ice cover on a boom, ice pressure against structure*. NRC Conference, Quebec, 1966.
[22] NVE (Norvegian Water Resources and Energy Administration), The Norvegian Dam Safety Project, Main Report, 1992.
[23] Liu, K.F., Lee, F.C. & Tsai, H.P., The flow field and impact force on debris dam, debris-flow hazards mitigation. *Proceedings of the 1st International Conference, ASCE, San Francisco*, pp. 737–743, 1997.
[24] Dudley, S.J., Fischenich, J.C. & Abt, S.R., Effect of woody debris entrapment on flow resistance. *Journal of the American Water Resources Association*, **34** (5), pp. 1189–1197, 1998.
[25] Michel, B., *Ice mechanics*. Presses de l'université Laval, 1978.
[26] Fuamba, M., Marche, C. & Quach, T. Ice-cover impact on dam-break wave propagation: experimental study (in French). Canadian Journal of Civil Engineering, **27** (5), 1082–1087, 2000.
[27] Fuamba, M., Bouaanani, N. & Marche, C., Modeling of dam break wave propagation in a partially ice-covered channel. *Advances in Water Resources*, **30**, pp. 2499–2510, 2007.
[28] Beltaos, S., *River ice jams*. Water Ressources Publications, LLC, USA, 1995.
[29] Bouaanani, N., Paultre, P. & Proulx, J., Two-dimensional modelling of ice-cover effects for the dynamic analysis of concrete gravity dams. *Journal of Earthquake Engineering and Structural Dynamics*, **31**, pp. 2083–2102, 2002.
[30] Cunge, J.A. & Wegner, M., Numerical integration of Barre de St Venant's flow equations by means of an implicit scheme of finite difference. Application in the case of alternately free and pressurized flow in a tunnel. *La Houille Blanche*, **1**, pp. 33–39.

[31] Singh, V.P., *Dam breach modelling technology.* Kluwer Academic, Dordrecht, Boston 1996.
[32] Visser, P.J., Breach growth in sand dikes. Communications on Hydraulics and Geotechnical Engineering, TU Delft, Report 98–1.
[33] Wurbs, R.A., Dam breach flood wave models. *Journal of Hydraulic Engineering*, **113** (1), pp. 29–46, 1987.
[34] IMPACT: Investigation of Extreme Flood Processes & Uncertainty, 2003, http://www.samui.co.uk/impact-project/.
[35] Marche C., Embankment dam overtopping and collapse: an innovative approach to predict the breach outflow hydrograph, Fluid structure interaction and moving Boundary problems. *WIT Transactions on the Built Environment*, **84**, pp. 119–130, 2005.
[36] Mahdi, T., Marche, C., Prévision par modélisation numérique de la zone de risque bordant un tronçon de rivière subissant une crue exceptionnelle. *Canadian Journal of Civil Engineering*, **30** (3), pp. 568–579, 2003.
[37] Noel, B., Soares-Frazao, S. & Zech, Y., Computation of the 'isolated buildind test case' and the model city experiment benchmarks, EC contract EVG1-CT-2001-00037 IMPACT Investigation of Extreme Flood Processes and Uncertainty. *Proceedings of the 3rd Project Workshop*, Louvain la Neuve, Belgium, 2003.
[38] Alcrudo, F, Garcioa P., Brufau, J., Murillo, D., Garcia, J. M., Testa, G. Zuccala, D., *The model city flooding experiment*. Impact project technical report. WP3_10 Summary, v1.0, 2004.
[39] Murillo, J., Mulet, J., Brufau, P., Garcia-Navarro, P. & Alcrudo, F., *The model city flooding experiment benchmark. Analysis of modeller's results and conclusions*, IMPACT project technical report. WP3_10 Summary_v1_0, 2004.
[40] Ferreira, R.M.L., River flow 2006. *Proceedings of the International Conference on Fluvial Hydraulics*, Lisbon, Portugal, 6–8 September 2006, Taylor & Francis group, London, 2006.
[41] Hervouet, J.M., Samie, R. & Moreau, B., Modelling urban areas in dam-break flood wave numerical simulations, *Proceedings of Rescdam Workshop*, Seinajoki, Finland, 2000.